Workshop on Binary and Variable Stars
Gunma Astronomical Observatory, 1999

Evolutionary Constraints Imposed by Pulsations in Extreme Helium Stars

Simon Jeffery

Armagh Observatory, College Hill, Armagh BT61 9DG, Northern Ireland

Abstract. Extreme helium stars are highly evolved luminous stellar remnants. Their exotic surface abundances point to previous evolution through the white dwarf sequence, followed by re-ignition due to a late helium shell flash or to a binary merger. The existence of pulsations in many helium stars, due to strange-mode instabilities or the Z-bump κ-mechanism, provide a range of diagnostics including radii from Baade's method and contraction rates from period changes. I review the basic observational and theoretical properties of extreme helium star pulsations and show how these have been used to constrain evolutionary models, with particular reference to the cases of V652 Her and BX Cir.

1. Extreme Helium Stars

The late stages of stellar evolution are characterized by extremes. Stellar structure and surface properties change much more rapidly than during earlier phases of evolution. A star will reach its highest luminosity and, often, its highest effective temperature shortly before it finally becomes a white dwarf. Mass-loss and mixing may expose highly-processed material on the stellar surface, resulting in the formation of chemically peculiar stars. The latter are distributed over most of the Hertzsprung-Russell diagram; one of the most extreme examples is provided by the extreme helium stars (EHes) – early-type supergiants practically void of hydrogen in their atmospheres.

The remarkable hydrogen-deficiency of an EHe is demonstrated by the weakness of its Hγ line. In the case of a normal B star, such as γ Peg, this typically broad line dominates the local spectrum. In the case of the extreme helium star LSE 78, Hγ is almost completely replaced by a blend of S III and O II absorption lines. The effective temperatures of these two stars are 21,500 K and 18,000 K respectively (Peters 1976, Jeffery 1993), so that the ionization balance of their photospheres will not be dissimilar. Hydrogen constitutes less than 10^{-5} parts by number in LSE 78. A direct consequence of the low hydrogen abundance is that the continuum opacity, normally dominated by hydrogen, is reduced. Although the abundances of species other than helium and carbon are not significantly different from solar, the metal line spectrum is correspondingly magnified several fold.

This paper introduces the principal properties of extreme helium stars. Since their surface compositions imply an unusual evolutionary history, I review the principal scenarios currently considered. Stellar mass is critical to a correct

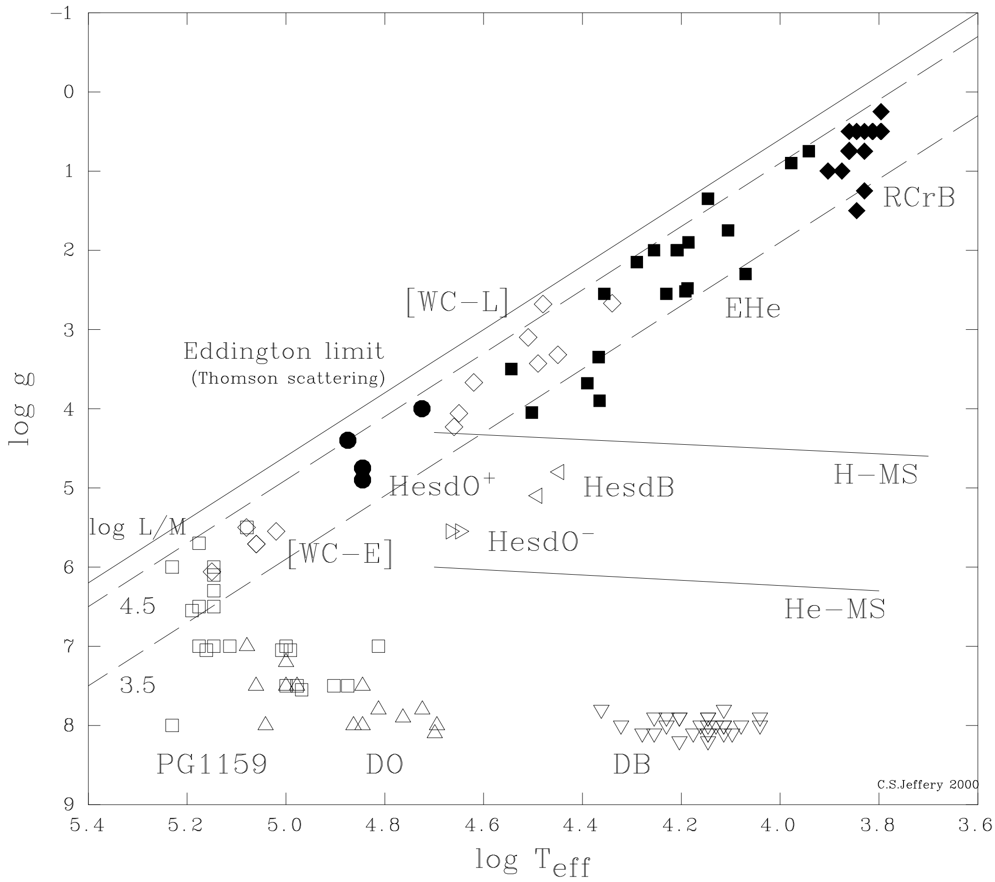

Figure 1. $T-g$ diagram for hydrogen-deficient stars including RCrB stars (⧫: Asplund et al. 2000), EHe stars (■: Jeffery 1996, Pandey 1999), low gravity helium-rich sdO stars (HesdO$^+$, •: Husfeld et al. 1989), [WC] stars (◇: Hamann 1996, assuming $M = 0.6\,\mathrm{M}_\odot$), PG1159 stars (□: Werner et al. 1996), high-gravity HesdO stars (HesdO$^-$, ◃: Dreizler 1993), helium-rich sdB stars (HesdB, ▹: Heber et al. 1988), DO white dwarfs (△: Dreizler & Werner 1996), and DB white dwarfs (▽: Wegner & Nelan 1987). The Eddington limit, loci of constant L/M, and hydrogen and helium main sequences (H-MS, He-MS) are also shown.

interpretation of stellar evolution, so methods for its measurement are compared. The importance of pulsations in providing masses and other characteristics of helium star evolution is demonstrated, with particular reference to the radial pulsations in V652 Her and BX Cir.

2. Stellar Properties

The characteristic surface properties, effective temperature T, surface gravity g and composition X, of EHes have been summarized by Jeffery (1996). The distribution of EHes in the $T - g$ plane is shown in Fig. 1 together with the location of other H-deficient stars, notably the putatively related RCrB stars. It may be seen that they lie roughly along a locus given by $\log L/M \sim 4$, which also corresponds to the evolution track of post-AGB stars, contracting towards the white dwarf track. This has guided most of discussion of their evolutionary status within the context of post-AGB evolution.

The surface compositions of EHes vary considerably from star to star, but may be briefly summarized as follows[1].

Hydrogen: ($-4.6 < \log n_{\rm H} < -0.8$) The fact that some hydrogen is found in the atmospheres of nearly all EHes indicates that some remnant of the outermost hydrogen-rich layers of the progenitor has been retained.

Helium: ($0.9 < n_{\rm He} < 1.0$) By definition, helium dominates the atmospheric abundances.

Nitrogen: ($0.4 < [N/Fe] < 1.2$) Nitrogen is enriched in most EHes, implying that helium has been produced by CNO cycling. If all nitrogen comes from such a source, it should reflect the total C+N(+O) abundances in the progenitor. This is supported by a correlation between N and Fe abundances in EHes.

Carbon: ($0.9 < [C/Fe] < 2.0$) Carbon is substantially enriched in nearly all EHes, indicating the presence of material processed through 3α helium burning.

Oxygen: ($-0.6 < [O/Fe] < 0.8$) Since $n_{\rm N}$ indicates the destruction of oxygen, nearly all observed oxygen has probably been produced by $^{12}{\rm C}(\alpha,\gamma)^{16}{\rm O}$. The O/C ratio should therefore provide a diagnostic of conditions in the C-rich layers of the progenitor. Observed O/C ratios do not approach the value expected in CO cores, except in two cases (DY Cen and LSE 78).

Iron: The iron abundances fall approximately into two groups (with the exceptions of DY Cen and HD144941) clustered about $[Fe] \sim 0.0 \pm 0.1$ and $[Fe] \sim -0.9 \pm 0.2$. It remains to be seen whether the bimodal distribution of iron abundances persists to the complete EHe sample.

Consequently, any model for the origin of EHes must result in a surface mixture which includes a remnant of the hydrogen envelope, predominantly CNO-processed helium and a significant quantity of 3α and $^{12}{\rm C}+\alpha$ products, as well as reproducing the overall dimensions such as luminosity, mass and effective temperature.

---

[1] Abundances are referred to as (i) $n_{\rm X}$ = relative abundance of species X by number, (ii) log $n_{\rm X}$ = log of above, (iii) $[X] = \log n_{\rm X}/n_{\rm X\odot}$, representing log abundance relative to solar and (iv) $[X/Fe] = \log(n_{\rm X}/n_{\rm Fe})/(n_{\rm X}/n_{\rm Fe})_\odot$, representing the same scaled to allow for the difference between the stellar and solar iron abundance.

3. Evolution Models

Several scenarios have been proposed to account for the depletion of surface hydrogen in extreme helium stars. Those which may be successful in producing extremely hydrogen-poor surfaces are the following:

Case BB mass transfer in a binary. Following main-sequence evolution, a red giant star in a close binary system may expand to fill its Roche lobe. Transferring mass to the less massive companion (Case B) will reduce but not remove the H-rich envelope. If core-helium burning is completed before the secondary completes its main-sequence evolution and the primary expands to the giant region for a second time, then a further phase of mass transfer (case BB) can completely remove the H-rich envelope, exposing CNO-processed helium (Plavec 1973, Schönberner & Drilling 1983). Although Iben & Tutukov (1984) used this model to account for the EHes, the latter are not binaries (Jeffery et al. 1987). Case BB mass transfer *does* account successfully for the observations of hydrogen-deficient binaries such as υ Sgr and KS Per.

Final helium-shell flash in a post-AGB star. The model proposed by Iben et al. (1983) derives from evolutionary calculations of post-AGB stars. At some point during contraction from the AGB to the white dwarf (WD) track, some models were found to experience a late thermal pulse – or helium-shell flash. The energy output of this last shell flash causes large-scale mixing and a brief expansion of the envelope to giant dimensions. Strong evidence that such late shell flashes do occur comes from three objects, V652 Aql, FG Sge and V4334 Sge, all of which have been observed to evolve from faint blue star to a red supergiant on timescales of 3 – 50 years. In the case of V652 Aql, contraction after the shell flash to the WD track was also rapid. Recently, more detailed evolutionary calculations have been carried out for WDs which experience a late shell flash (Herwig et al 1999). The post-expansion tracks have been compared favourably with observations of other H-deficient objects including some central stars of PN ([WC] stars) and very hot pre-WDs (PG1159 stars). All of these objects have a surface carbon abundance of $\sim 10\%$ or greater. If the final shell-flash model successfully explains such stars, the question is whether it can also explain EHes, with $\sim 1\%$ carbon abundances and apparently slower evolutionary timescales.

Merger of CO and He white dwarf. While most proposed models for EHes invoke post-AGB evolution, the model introduced by Webbink (1984) is completely different. A binary system with appropriate initial masses and orbital separation can evolve to the point where both stars are WDs, one being a carbon-oxygen WD of $\sim 0.6\,M_\odot$, the other a helium WD of 0.3–0.4 $M_\odot$, with an orbital period in the range 1–10 hours. Over a long interval, the orbital angular momentum can be reduced by a combination of gravitational-wave radiation and magnetic-wind braking to the point at which the less massive WD fills its Roche lobe. Tidal disruption will follow on a dynamical timescale, the WD being transformed into a thick disk around the more massive companion. Accretion from the disk onto the surviving WD creates a star with a degenerate CO core and a helium envelope. Depending on the accretion rate, helium may be ignited either explosively (slow accretion) or quiescently (fast accretion), resulting in either a type

Ib supernova or a helium giant (Iben & Tutukov 1985). Numerical models for the mergers of two CO WDs and two He WDs have been computed (Saio & Nomoto 1998, Saio & Jeffery 2000), but the CO+He case has yet to be treated successfully.

Other models. Schönberner (1986) discusses a variety of unsuccessful models which have been proposed at one time or another. Only the final-flash and WD-merger models currently seem capable of reproducing most of the observed properties of EHes.

4. Masses

To test whether any evolutionary model is correct, reliable tests are required. These include a detailed comparison between models which predict evolution tracks and surface composition for a given stellar mass and accurate observations of stellar compositions and dimensions. Stellar compositions, temperatures and gravities can be measured relatively simply, but measuring mass is less straightforward. There are three principal approaches.

Spectroscopic Mass $M_{\rm S}$. Suppose some physical mechanism connects the mass M of the star to its luminosity L, such as the mass-luminosity relation for main-sequence stars or a core-mass shell-luminosity relation for shell-burning stars. From spectroscopy and model atmospheres, the effective temperature T and surface gravity g of the star can be measured. Since $L/M \propto T^4/g$, then the spectroscopic mass $M_{\rm S}$ of the star may be deduced using an appropriate $M-L$ relation (e.g. Jeffery 1988).

Pulsation Mass $M_{\rm P}$. Stellar pulsations provide much more powerful tools for determining stellar masses. Fortuitously, pulsations appear to be common amongst EHes (see next section). The most straightforward approach is provided by pulsation periods Π obtained from photometry. Linear theory provides theoretical pulsation periods for stellar models of given M, T and L. In conjunction with spectroscopic measurements of T and g, Π can provide an estimate of the pulsation mass $M_{\rm P}$.

Direct Mass $M_{\rm D}$. In some cases, it may be possible to measure the angular radius (θ) and radial velocity (v) of a pulsating stars throughout the pulsation cycle. v may be integrated to yield the total radius change δR. $\delta\theta/\theta$ gives the relative radius change. The stellar radius R is then given by $R = \delta R/(\delta\theta/\theta)$. Following Baade (1926) and combining the radius with g from spectroscopy and model atmospheres yields the direct mass $M_{\rm D} \propto g/R^2$.

5. Pulsation Properties

Although pulsations in EHes appear to be ubiquitous, it is not possible to summarize their properties with a single definition. Three groups may be identified; future observations will no doubt add to these.

V652 Her variables – "Z-bump" pulsators. The first discovery of pulsation in an EHe was made by Landolt (1975), who discovered a 0.1 day photometric period in V652 Her, and by Hill et al. (1981), who measured the radial velocity curve and demonstrated the variations were due to radial pulsation. The pulsation is strictly periodic with regular light and radial-velocity curves. The discovery enabled Lynas-Gray et al. (1984) to deduce a direct mass $M_{\rm D} = 0.7^{+0.4}_{-0.3}\,{\rm M}_{\odot}$, whilst Kilkenny & Lynas-Gray (1982) discovered that the pulsation period was shrinking in a manner consistent with a secular contraction. These properties will be examined later.

Radial pulsations are mostly driven by the κ mechanism. This occurs in a zone which gains thermal energy as it is compressed and loses thermal energy as it expands. A zone gains thermal energy if the incoming radiation flux at the lower boundary exceeds the outgoing flux at the upper boundary, i.e. the radiation flux is blocked. This occurs if the increase in opacity caused by the compression increases outwards, i.e. ${\rm d}[\delta\kappa]/{\rm d}r > 0$. The opacity variation due to a nearly adiabatic pulsation is given as

$$\delta\kappa = \frac{\partial\kappa}{\partial\rho}\delta\rho + \frac{\partial\kappa}{\partial T}\delta T = \left[\frac{\partial\kappa}{\partial\rho}\left(\frac{{\rm d}\rho}{{\rm d}T}\right)_{\rm ad} + \frac{\partial\kappa}{\partial T}\right]\delta T.$$

Therefore, neglecting the spatial variation of δT, ${\rm d}[\delta\kappa]/{\rm d}r > 0$ when $\delta T > 0$ (i.e. compression) is an approximate formal condition for κ-mechanism driving in nearly adiabatic pulsations. The occurrence of strong opacity peaks at an appropriate depth in the stellar envelope is an important criterion for such pulsations. In classical Cepheids, with $T \sim 7,000\,{\rm K}$, driving is provided by the He II opacity peak at $\sim 40,000\,{\rm K}$.

Prior to 1990, all attempts to model the pulsation in V652 Her found the star to be stable. While stars hotter than the classical Cepheid instability strip could show radial pulsations, this was only true if they were considerably more luminous than V652 Her (Saio & Jeffery 1988, see below). This problem was overcome with the calculation of stellar opacities which more correctly included the contribution of iron-group elements at temperatures around 2×10^5 K (Rogers & Iglesias 1992, Seaton et al. 1994). The opacity peak due to iron-group elements, often referred to as the "Z-bump", can have a similar effect to the He II opacity peak at lower temperatures, particularly if the hydrogen-abundance is low. Saio (1993) showed that a 'finger of instability' exists for helium stars with $T \sim 20\,000\,{\rm K}$ and which also have a sufficiently high metallicity and luminosity, such as V652 Her.

V652 Her lies right in the middle of this finger of instability, as do two other stars: HD144941 and LSS 3184. If "Z-bump" instability was responsible for pulsations in V652 Her, then these other stars should also pulsate with similar periods $\sim$ 0.1 day. Observations of HD144941 failed to find any evidence of variations (Jeffery & Hill 1996), but this was easily explained by its very low metallicity $Z = 0.0003$ (Harrison & Jeffery 1997, Jeffery & Harrison 1997). Prompted by Saio's (1995) prediction, Kilkenny & Koen (1995) discovered a 0.1 day photometric period in LSS 3184=BX Cir and with radial velocities the radial pulsations have been more fully characterized by Kilkenny et al. (1999). The metallicities of V652 Her and BX Cir have been measured as $Z = 0.016$ (Jeffery et al. 1999) and $Z = 0.007$ (Drilling et al. 1998) respectively.

Jeffery & Saio (1999) have explored the extent of the Z-bump instability finger for radial and non-radial pulsations in terms of mass, metallicity and hydrogen abundance and have shown that it is principally quenched if metallicity is too low ($Z \lesssim 0.002$) or if the hydrogen abundance is too high ($X \gtrsim 0.5$), for masses in the range 0.3–0.9 $\mathrm{M}_{\odot}$. Since other hot helium-rich subdwarfs lying close to this Z-bump finger are known, it is possible that more V652 Her variables remain to be discovered.

PV Tel variables – radial "strange" mode pulsators. One of the brightest EHes, PV Tel was considered to show irregular brightness and radial velocity variations on timescales of weeks, months and years (Walker & Hill 1985). More systematic observations of another EHe, FQ Aqr, led to the discovery of small-amplitude ($\sim 0^{\mathrm{m}}.1$) photometric variations with an apparent period of about 21 day (Jeffery & Malaney 1985). Subsequent observations confirmed the variations, but the period was ambiguous (Jeffery et al. 1986). More recently, five years worth of data demonstrated that variations persist on a characteristic timescale of $\sim$ 21 day, but with no long-lasting *coherent* period (Kilkenny et al. 1999). These variations are accompanied by small-amplitude velocity variations of a few $\mathrm{km\,s^{-1}}$(Lawson et al. 1993).

Similar properties have since been detected in a number of other EHes including PV Tel, NO Ser, V2244 Oph, V354 Nor and V1920 Cyg (cf. Lawson et al. 1993). This group all have $8\,000 \leq T/\,\mathrm{K} \leq 15\,000$, low surface gravities and $7 \leq \Pi/\,\mathrm{day} \leq 25$, where Π here represents the characteristic timescale.

Variability of similar character but longer Π has been recorded in RCrB stars and associated with radial pulsations for some time. These pulsations are reviewed by Lawson & Kilkenny (1996). Whilst RCrB pulsators are relatively cool, EHes are considerably hotter than, for examples, classical Cepheids. Lying to the blue of the classical instability strip, their pulsations are a consequence of the extremely non-adiabatic conditions in the envelopes of stars with high L/M ratios. Dubbed 'strange' modes, the pulsations are primarily associated with regions of density inversion, such as the He II ionization zone (Saio et al. 1998). Strange modes are characteristically different to κ-modes since their frequencies change rapidly with stellar parameters (e.g. M, T). For EHes and RCrBs, two consequences noted by Saio & Jeffery (1998) are that (i) the stability criterion is effectively provided by the L/M ratio, and (ii) Π and T are related approximately linearly.

The extreme non-adiabacity of EHe envelopes provides a possible explanation for their quasi-periodic behaviour. If the start and end states for each pulsation cycle are not identical, each cycle will not resemble the previous cycle exactly in either amplitude or duration. Over time, the oscillation will forget its history or, effectively, lose phase coherence, even though the local characteristic timescale will be unchanged[2]. The failure of nonlinear calculations of RCrB models to show limit cycles (Saio & Wheeler 1985) supports this proposal, whilst Fadeyev (1993) found considerable disagreement between the results of linear and non-linear calculations. Further non-linear calculations for PV Tel

[2] This is actually the description of chaotic behaviour in a mechanical system.

and RCrB variables are required.

V2076 Oph variables – non-radial "strange" mode pulsators. The most luminous EHes with $T > 20\,000\,\mathrm{K}$ are also small-amplitude variables. The light curves of V2076 Oph and V2205 Oph are considerably more complicated than those of the PV Tel variables and have shorter characteristic timescales of $0.7 - 1.1$ day and $3 - 9$ day respectively (Lynas-Gray et al. 1987, Jeffery et al. 1985). It appears that the variations are multi-periodic, and that the characteristic timescales are longer than anticipated for radial fundamental or first harmonic pulsations. The conclusion is that both stars pulsate non-radially, possibly in a low-order g-mode. Radial velocity measurements support this conclusion, with line-profile variations in V2205 Oph indicating $m = -2, l = 2$ or 3 (Jeffery & Heber 1992).

Linear radial pulsation theory indicates that these stars should be unstable to strange-mode pulsations. However, the most unstable radial mode is no longer similar to the fundamental or first harmonic, but a much higher-order mode (Saio & Jeffery 1988). Glatzel & Gautschy (1992) investigated non-adiabatic non-radial pulsations in a limited helium star evolution sequence, and found strange-mode instabilities at temperatures up to the limit of their study at $T \sim 20\,000\,\mathrm{K}$. The similar appearance of the instabilities for radial and non-radial pulsations suggests that non-radial strange-modes may be responsible for the variability in V2076 Oph and V2205 Oph. However the models used by Glatzel & Gautschy (1992) are less evolved than these stars are likely to be. An important experiment will be to perform linear non-radial pulsation analyses for any evolution models constructed to explain the origin of these EHes.

A major observational difficulty concerns both the multi-periodicity and the extreme non-adiabacity of the pulsations. Existing observations need to be substantially improved both in sampling rate and duration in order to fully resolve the frequency structure of the light curves. However, if the quasi-periodicity of radial pulsations in cooler stars extends to the hotter non-radial counterparts, frequency analyses of long data trains will be doomed from the outset. The observation and modelling of non-radial pulsations in extremely luminous stars (including EHes) presents a major challenge for astrophysics.

6. V652 Her and Merged Binary White Dwarf Models

As already indicated, V652 Her is an important EHe star because its relatively short pulsation period and large amplitude pulsations allow its overall dimensions to be determined with high precision. The pulsation properties have been determined from visual and ultraviolet spectrophotometry and from spectroscopy by Landolt (1975), Hill et al. (1981), Lynas-Gray et al (1984) and Jeffery & Hill (1986). The simple saw-tooth shape of the radial-velocity curve implies that the pulsation can be divided quite simply into a short impulse phase lasting < 0.1 cycles, followed by a near free-fall phase for the remainder of the cycle. Combining these data, Lynas-Gray et al. (1984) obtained a direct measurement of the radius $R = 2.0 \pm 0.2\,\mathrm{R}_\odot$ and mass $M_\mathrm{D} = 0.7^{+0.4}_{-0.3}\,\mathrm{M}_\odot$. A refinement of the measurement of g led Jeffery et al. (1999) to obtain $M_\mathrm{D} = 0.69 \pm 0.15\,\mathrm{M}_\odot$, with $T = 24\,450 \pm 500\,\mathrm{K}$, $\log g = 3.68 \pm 0.05$ (cgs) and $L \sim 10^3\,\mathrm{L}_\odot$. In contrast to most EHes, V652 Her is nitrogen rich and carbon and oxygen poor, implying

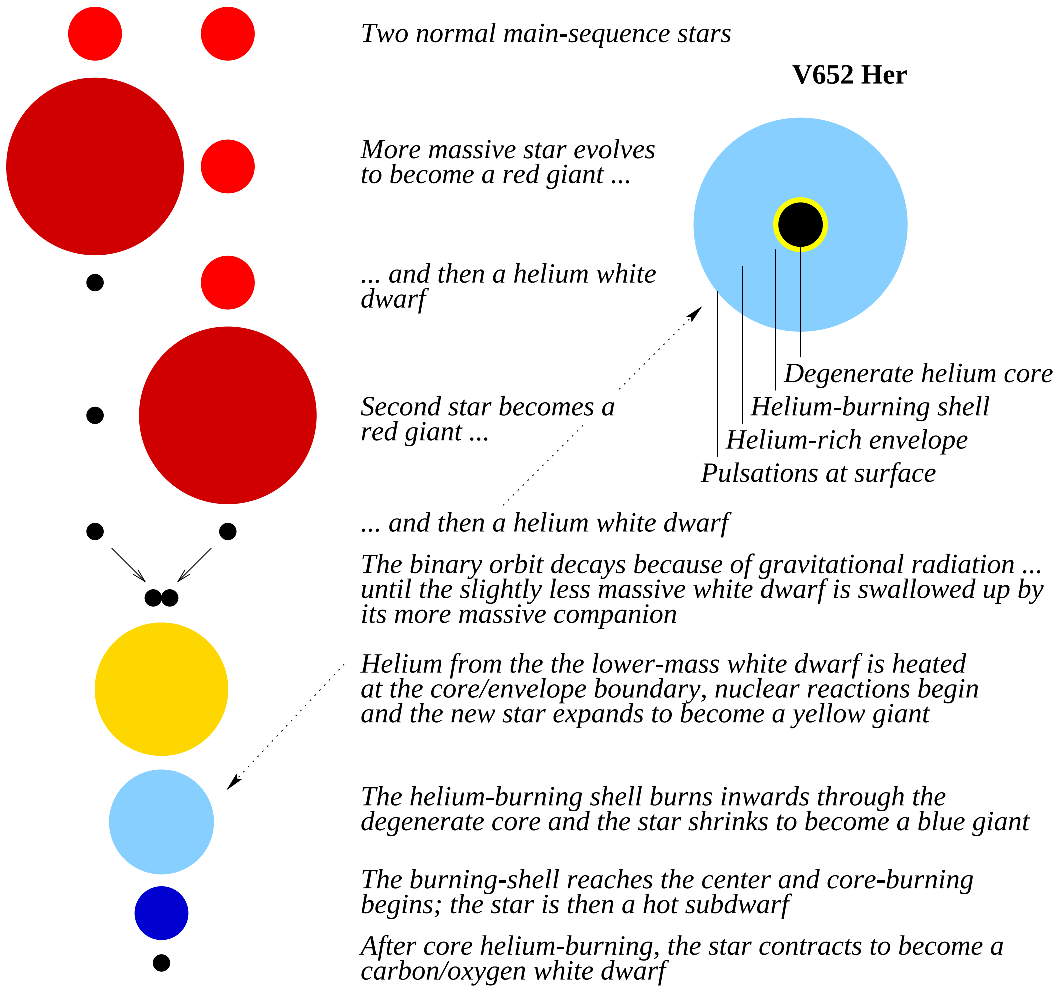

Figure 2. Illustration of the merged-binary white dwarf evolution model for V652 Her (Saio & Jeffery 2000).

that its surface is predominantly CNO-processed. The period change discovered and refined by Kilkenny & Lynas-Gray (1982,1984) and Kilkenny et al. (1996) translates into a contraction rate $\dot{R}/R \sim 2.10^{-4}\,\text{yr}^{-1}$, together with nonlinear terms $\ddot{R}$ and $\dddot{R}$.

With a lower luminosity and a purely CNO-processed surface, the evolutionary status of V652 Her has long been regarded as possibly quite different to most EHes. Jeffery (1984) constructed a set of highly artificial "helium horizontal branch models" in which a $0.5\,M_\odot$ helium-burning core was surrounded by an envelope with a very low hydrogen abundance. Because of the low hydrogen-abundance, the luminosity of the H-burning shell at the core-envelope interface was very high and the star evolved rapidly towards the helium main-sequence. Whilst able to match $M, L, T, \dot{R}$ and surface composition, these models could only suggest a possible structure for V652 Her, rather than explain its origin.

Other highly artificial models in the horizontal-branch family have been constructed, notably by Sweigart (1997), but fail to provide either a hydrogen-poor surface or a self-consistent explanation of their origin. Similarly, no "final-flash" models have been computed which match the observed properties of V652 Her.

Saio & Nomoto (1998) made the first successful models for the merger of two carbon-oxygen white dwarfs, and prompted Saio & Jeffery (2000) to attempt models for the merger of two helium white dwarfs. Following orbital decay, the less massive white dwarf in a double-degenerate suffers total tidal disruption on a dynamical timescale; the debris forms a thick disk around the surviving white dwarf. The latter then accretes matter from the disk until the envelope is sufficiently massive that nuclear reactions, in this case 3α burning, are initiated at the core-envelope interface. At this point, the star expands to become a cool helium giant. Heating of the core surface by the nuclear-burning shell, or flame, lifts the local electron-degeneracy so that the flame migrates inwards. Because the flame migration proceeds stepwise, the surface evolution follows a series of loops of increasing T and decreasing L, until the flame reaches the core centre, whereupon the star assumes the structure of a helium main-sequence star or hot subdwarf. A schematic of the evolution is shown in Fig. 2.

The evolution sequence for a $0.476\,\mathrm{M}_\odot$ helium white dwarf accreting $0.233\,\mathrm{M}_\odot$ helium-rich debris passes exactly through the observed locus for V752 Her. To within the numerical uncertainty of the calculations, this model also has the correct pulsation properties, Π and $\dot{\Pi}$. As yet, the higher order terms $\ddot{R}$ and $\dddot{R}$ (Kilkenny et al. 1996) cannot be reproduced.

Table 1. Mass estimates (in $\mathrm{M}_\odot$) for PV Tel variables from (i) spectroscopy M_S using the $M_\mathrm{c} - L_\mathrm{s}$ relation from Jeffery (1988), (ii) pulsation periods M_P (Saio & Jeffery 1988) and (iii) direct measurement M_D (Jeffery et al. 2000).

Star	M_S	M_P	M_D
HD168476=PV Tel	0.95	0.85	0.82
BD+1°4381=FQ Aqr	1.09	0.93	0.03
LS IV−1°2=V2244 Oph	0.66	0.94	0.76

7. Direct Masses for BX Cir and PV Tel Variables

The discovery of BX Cir with properties very similar to V652 Her and the subsequent analysis of its light and velocity curves gave Kilkenny et al. (1999) the opportunity to derive its radius using Baade's method. However, in conjunction with the Drilling et al. (1998) value for $\log g$, their results yielded $M_\mathrm{D} = 0.15\,\mathrm{M}_\odot$, a value that is difficult to accept. A new study using AAT échelle spectroscopy and HST spectrophotometry promises to revise this value upwards (Woolf & Jeffery, in preparation).

Measuring M_D for the PV Tel variables poses considerable difficulties. Since the pulsations are not strictly regular, comparing angular and radial variations

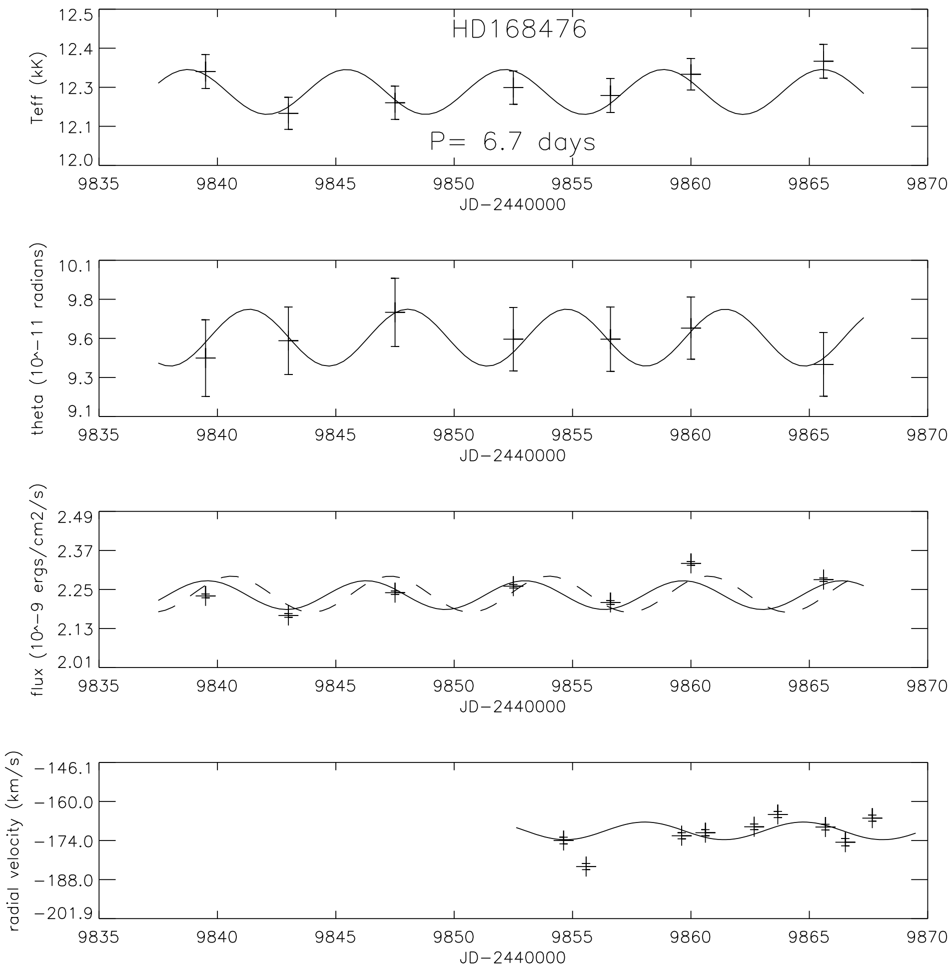

Figure 3. The ultraviolet and radial velocity behaviour of HD168476=PV Tel (from Jeffery et al. 2000). From top to bottom, the four panels show the variation of $T_{\rm eff}$, θ, $F_{\rm IUE}$ and v. Superimposed on each is a sine curve; the period for all four fits is indicated in the top panel, the phase and amplitude were obtained from an independent least-squares fit to each set of data (solid curves). The dashed curve represents the product of the fits $\theta^2\ {T_{\rm eff}}^4$ scaled to the same mean value as $F_{\rm IUE}$.

requires that observations be obtained simultaneously. Moreover the radial-velocity amplitudes are small, the periods are long, and ultraviolet photometry is essential. In spite of these constraints, Jeffery et al. (2000) succeeded in obtaining nearly contiguous ultraviolet photometry and radial velocities (v) of three PV Tel variables. Analysis of the UV photometry provides measures of T, θ and Π. Fitting θ and v with sine curves provides estimates of their mean amplitudes, and hence their mean radii. The data for PV Tel is shown in Fig. 3. These provided remarkably convincing estimates of $M_{\rm D}$ in two cases, albeit with significant errors. The failure of the method in the third case (FQ Aqr) could be a consequence of its low T, but highlights the fact that the data are far from ideal. It is interesting to compare the three masses $M_{\rm S}, M_{\rm P}, M_{\rm D}$ for the three PV Tel variables in our sample (table 1).

8. Summary

The highly-processed surfaces of extreme helium stars point to an extremely unusual evolutionary history. In order to test candidate theories it is necessary to make reliable measurements of, in particular, stellar masses. Three methods are available; all depend on a measurement of the surface gravity g. The spectroscopic mass $M_{\rm S}$ requires a suitable mass-luminosity relation. The pulsation mass $M_{\rm P}$ is obtained from a pulsation period and linear pulsation theory, and the direct mass $M_{\rm D}$ is provided directly by the pulsation properties.

Data now exists to provide direct masses for five EHes. That for V652 Her is well established and agrees well with evolution models involving the merger of two helium white dwarfs. The result demonstrates that pulsations are an essential and successful tool for determining the evolutionary origin of extreme helium stars.

Direct masses for PV Tel and V2244 Oph agree well with the spectroscopic and pulsation masses, although much may be done to reduce the errors. Further painstaking observations and analyses are also required for BX Cir and FQ Aqr.

Acknowledgments

The author is grateful to the organizers of the Workshop on Binary and Variable Stars for their kind invitation to give this review, and to Hideyuki Saio and Vincent Woolf for their critical comments on the manuscript. The British Council and the Japanese Society for the Promotion of Science have sponsored some of the research reviewed through their UK – Japan Exchange Programmes in Science & Technology.

References

Asplund M., Gustafsson B., Lambert D.L., Rao N.K., 2000. A&A 353, 287
Baade W., 1926. Astr. Nachr., 228, 359
Dreizler S., 1993. A&A 273, 212
Dreizler S., & Werner K., 1996. Hydrogen-deficient stars, eds. C.S.Jeffery, U.Heber, ASP Conf Ser. 96, 281
Drilling J.S., Jeffery C.S., Heber U., 1998. A&A 329, 1019

Fadeyev Yu.A., 1993. MNRAS 262, 119
Glatzel W., Gautschy A., 1992. MNRAS 256, 209
Hamann W.-R., 1996. Hydrogen-deficient stars, eds. C.S.Jeffery, U.Heber, ASP Conf Ser. 96, 127
Harrison P.M., Jeffery C.S., 1997. A&A 323, 177
Heber U., Dreizler S., de Boer K.S., Moehler S., Richtler T., 1988. Astron. Ges. Abs. Ser. 1, 16
Herwig F., Blöcker T., Langer N., Driebe T., 1999. A&A 349, L5
Hill P.W., Kilkenny D., Schönberner D., Walker H.J., 1981. MNRAS 197, 81
Husfeld D., Butler K., Heber U., Drilling J.S., 1989. A&A 222, 150
Iben I.,Jr., Kaler J.B., Truran J.W., Renzini A., 1983. ApJ 264, 605
Iben I.,Jr., Tutukov A., 1984. ApJ 284, 719
Iben I.,Jr., Tutukov A., 1985. ApJS, 58, 661
Jeffery C.S., 1984. MNRAS 210 731
Jeffery C.S., 1988. MNRAS 235, 1287
Jeffery C.S., 1993. A&A 279, 188
Jeffery C.S., 1996. Hydrogen-deficient stars, eds. C.S.Jeffery, U.Heber, ASP Conf Ser. 96, 152
Jeffery C.S., 1998. MNRAS 294, 391
Jeffery C.S., Drilling J.S., Heber U., 1987. MNRAS 226, 317
Jeffery C.S., Hamill P.J., Harrison P.M., Jeffers S.V., 1998. A&A 340, 476
Jeffery C.S., Harrison P.M., 1997. A&A 323, 393
Jeffery C.S., Heber U., 1992. A&A 260, 133
Jeffery C.S., Heber U., 1993. A&A 270, 167
Jeffery C.S., Hill P.W., 1986. MNRAS 221, 975
Jeffery C.S., Hill P.W., 1996. Observatory 116, 156
Jeffery C.S., Hill P.W., Heber U., 1999, A&A 346,
Jeffery C.S., Hill P.W., Morrison K., 1986. Hydrogen-deficient stars and related objects, eds. K.Hunger, D.Schönberner, N.K.Rao, Reidel, Dordrecht, IAU Coll. 87, 95
Jeffery C.S., Malaney R.A., 1985. MNRAS 213, 61P
Jeffery C.S., Saio H., 1999. MNRAS 308, 221
Jeffery C.S., Skillen I., Hill P.W., Kilkenny D., Malaney R.A., Morrison K., 1985. MNRAS 217, 701
Jeffery C.S., Starling, R.L.C., Hill P.W., Pollacco D., 2000. MNRAS submitted
Kilkenny D., Koen C., 1995. MNRAS 275, 327
Kilkenny D., Koen C., Jeffery C.S., Hill N.C., O'Donoghue D., 1999. MNRAS 310, 1119
Kilkenny S., Lawson W.A., Marang F., Roberts G., van Wyk F., 1999. MNRAS 305, 103
Kilkenny D., Lynas-Gray A.E., 1982. MNRAS 198, 873
Kilkenny D., Lynas-Gray A.E., 1984. MNRAS 208, 673
Kilkenny D., Lynas-Gray A.E., Roberts G., 1996. MNRAS 283, 1349
Landolt A.U., 1975. ApJ 196, 787
Lawson W.A., Kilkenny D., 1996. Hydrogen-deficient stars, eds. C.S.Jeffery, U.Heber, ASP Conf Ser. 96, 349
Lawson W.A., Kilkenny D., van Wyk F., Marang F., Pollard K., Ryder S.D., 1993. MNRAS 265, 351
Lynas-Gray A.E., Schönberner D., Hill P.W., Heber U., 1984. MNRAS 209, 387
Lynas-Gray A.E., Kilkenny D., Skillen I., Jeffery C.S., 1987. MNRAS 227, 1073
Pandey G., 1999. PhD Thesis, Indian Institute of Astrophysics.
Plavec M.J., 1973, in 'Extended Atmospheres ... ', p.216, ed. A.H.Batten, Dordrecht, Reidel
Rogers F.J., Iglesias C.A., 1992. ApJS 79, 507
Saio H., 1988. MNRAS 235, 203
Saio H., 1993. MNRAS 260, 465
Saio H., 1995. MNRAS 277, 1393

Saio H., Baker N.H., Gautschy A., 1998. MNRAS 294, 622
Saio H., Jeffery C.S., 1988. ApJ 328, 714
Saio H., Jeffery C.S., 2000. MNRAS (in press)
Saio H., Nomoto K., 1998. ApJ 500, 388
Saio H., Wheeler J.C., 1985. ApJ 295, 38
Schönberner D., Drilling J.S, 1983. ApJ 268, 225
Schönberner D., 1986. Hydrogen-deficient stars and related objects, eds. K.Hunger, D.Schönberner, N.K.Rao, Reidel, Dordrecht, IAU Coll. 87, 471
Seaton M.J., Yan Y., Mihalas D., Pradhan A.K., 1994. MNRAS 266, 805
Sweigart A.V., 1997. ApJ 474, L23
Walker H.J., Hill P.W., 1985. A&AS 61, 303
Webbink R.F., 1984. ApJ 277, 355
Wegner G., & Nelan E.P., 1987. ApJ 319, 916
Werner K., Dreizler S., Heber U., Rauch T., 1996. Hydrogen-deficient stars, eds. C.S.Jeffery, U.Heber, ASP Conf Ser. 96, 267